MYELOID NEOPLASIA

The human *NPM1* mutation A perturbs megakaryopoiesis in a conditional mouse model

Paolo Sportoletti,[1] Emanuela Varasano,[1] Roberta Rossi,[1] Oxana Bereshchenko,[2] Debora Cecchini,[1] Ilaria Gionfriddo,[1] Niccolò Bolli,[1] Enrico Tiacci,[1] Tamara Intermesoli,[3] Pamela Zanghì,[3] Arianna Masciulli,[4] Maria Paola Martelli,[1] Franca Falzetti,[1] Massimo F. Martelli,[1] and Brunangelo Falini[1]

[1]Institute of Hematology, and [2]Section of Pharmacology, University of Perugia, Perugia, Italy; [3]Hematology and Bone Marrow Unit, Ospedali Riuniti, Bergamo, Italy; and [4]Consorzio Mario Negri Sud, Santa Maria Imbaro, Italy

Key Points

- The NPM1 mutant affects megakaryocytic development in mice.
- NPMc$^+$ mutant mice mimic some features of human NPM1-mutated AML.

The *NPM1* mutation is the most frequent genetic alteration thus far identified in acute myeloid leukemia (AML). Despite progress in the clinical and biological characterization of *NPM1*-mutated AML, the role of *NPM1* mutation in leukemogenesis in vivo has not been fully elucidated. We report a novel mouse model that conditionally expresses the most common human *NPM1* mutation (type A) in the hematopoietic compartment. In *Npm1-TCTG/WT;Cre*$^+$ mice, the NPM1 mutant localized in the cytoplasm (NPMc$^+$) of bone marrow (BM) cells. The mutant mice developed no AML after 1.5-year follow-up. However, NPMc$^+$ expression determined a significant platelet count reduction and an expansion of the megakaryocytic compartment in the BM and spleen. Serum thrombopoietin levels overlapped in mutant vs control mice, and BM cells from *Npm1-TCTG/WT;Cre*$^+$ mice formed more megakaryocytic colonies in vitro. Moreover, we demonstrated the up-regulation of microRNAs (miRNAs; *miR-10a, miR-10b,* and *miR-20a*) inhibiting megakaryocytic differentiation along with increased expression of *HOXB* genes. Notably, these findings mimic those of human *NPM1*-mutated AML, which also exhibits a similar miRNA profile and expansion of the megakaryocytic compartment. Our mouse model provides evidence that the NPM1 mutant affects megakaryocytic development, further expanding our knowledge of the role of NPM1 mutant in leukemogenesis. (*Blood*. 2013;121(17):3447-3458)

Introduction

The *NPM1* mutation is the most frequent genetic alteration thus far identified in acute myeloid leukemia (AML), accounting for ~30% of all cases.[1] This mutation is highly stable over time and defines a subgroup of AML with distinctive clinico-pathological features and immunophenotype (including negativity for CD34)[2] and a relatively good prognosis in the absence of FMS-like tyrosine kinase 3 internal tandem duplication (FLT3-ITD) mutations.[3,4] Moreover, *NPM1*-mutated AML associates with a unique gene expression profile (including up-regulation of *HOX* genes)[5,6] and microRNA (miRNA) signature (including overexpression of *miR10a*, *miR10b*, and *miR20a*).[7-10] These features and the recent demonstration that leukemic stem cells isolated from *NPM1*-mutated AML patients carry the *NPM1* mutation[11] point to the latter as a founder genetic event.[12] Thus, *NPM1*-mutated AML is now listed as a provisional entity in the 2008 WHO classification of the lympho-hematopoietic neoplasms.[13]

The wild-type NPM1 protein shuttles between the nucleus and cytoplasm,[14] but, at the immunohistochemistry level, it mainly concentrates in the nucleolus.[15] Notably, all molecular variants of the *NPM1* mutation[12] result in critical changes at the C terminus of NPM1[16,17] that interfere with its nucleo-cytoplasmic traffic.[18] This leads to the aberrant accumulation of nucleophosmin in the cytoplasm of the leukemic cells (thus the term NPM cytoplasmic positive NPMc$^+$ AML).[19] The cytoplasmic dislocation of nucleophosmin appears to be critical to its leukemogenic activity.[18,20] The increased NPM1 export into the cytoplasm can affect multiple cellular pathways and may drive leukemia by either loss-of-function or gain-of-function mechanisms.[18] Indeed, many NPM1 interactors such as p19Arf[21] and Fbw7γ[22] can be delocalized into the cytoplasm by NPM1c$^+$, and their activity can be significantly impaired. Additionally, the NPM1 mutant has been described to interact and inhibit the cell death activity of caspase 6 and 8 in the cytoplasm.[23]

Despite the progresses in the biological and clinical characterization of *NPM1*-mutated AML,[2] the role of *NPM1* mutations in AML development in vivo is currently under investigation. A transgenic mouse model showed that the NPM1 mutant was implicated in abnormal myelopoiesis but not in progression toward leukemia.[24] In zebrafish, ubiquitous NPM1 mutant expression caused primitive myeloid cells expansion and increased the number of definitive *erythro*-myeloid progenitors cells.[25] Recently, Vassiliou et al[26] reported a knock-in mouse of human *NPM1* mutation A that, combined with insertional mutagenesis in vivo, identified genetic pathways collaborating with the NPM1 mutant in leukemogenesis. Nevertheless, the direct mechanism of action of the NPM1 mutant remains to be fully elucidated, and alternative gene-targeting approaches are still needed to study in vivo novel molecular mechanisms for *NPM1*-mutated AML.

Submitted August 10, 2012; accepted February 13, 2013. Prepublished online as *Blood* First Edition paper, February 22, 2013; DOI 10.1182/blood-2012-08-449553.

The online version of this article contains a data supplement.

The publication costs of this article were defrayed in part by page charge payment. Therefore, and solely to indicate this fact, this article is hereby marked "advertisement" in accordance with 18 USC section 1734.

To this end, we generated and characterized a mouse model that expresses the most frequent human *NPM1* mutation (type A) in hematopoietic stem cells. Our results show that the NPM1 mutant affects megakaryocytic development in mice and mimics some features of human *NPM1*-mutated AML.

Methods

This study was approved by the Institutional Review Board and conducted in accordance with the Declaration of Helsinki.

Generation and genotyping of mice with human *NPM1* mutation A

The human *NPM1* mutation A mouse was generated in collaboration with genOway (Lyon, France). The targeting vector was obtained by inserting the transgenic cassette expressing the human *NPM1* complementary DNA (cDNA) with mutation A into genOway's Rosa26 "quick Knock-in" targeting vector (G220 validation plasmid). This mutation consists of TCTG duplication at positions 956 to 959 of exon 12 of the reference sequence (GenBank accession number NM_002520) and represents the most frequent type of mutations of the *NPM1* gene in AML (~80% of cases).[1] The *NPM1* mutation cDNA fragment was subcloned into *Apa*I/*Hin*cII sites of a Tg-MSC plasmid containing the human growth hormone polyA. Then a *Mlu*I/*Sma*I fragment containing the *NPM1* mutation was cloned into the G220 plasmid. The G220 vector already contained the CAG promoter (a fusion of the cytomegalovirus immediate early enhancer and the chicken β-actin promoter)[27] with the downstream *lox*P flanked combined STOP-neomycin selection cassette.[28] Southern blotting and polymerase chain reaction (PCR) analyses were performed to genotype mice. For a record of primers used, see supplemental Materials on the *Blood* website.

Induction of Mx1-Cre expression in *Npm1-TCTG/WT*

Mice with the *NPM1* mutation A were bred with *Mx1-Cre* transgenic mice (Jackson Laboratory, Bar Harbor, ME) to generate *Npm1-TCTG/WT;Cre*$^+$ mice. Expression of Mx1-Cre and excision of PGK-Neo cassette were induced by polyinosinic-polycytidylic acid (pIpC) treatment in vivo. In brief, 8- to 12-week-old *Npm1-TCTG/WT;Cre*$^+$ mice were injected intraperitoneally with 250 μg/dose pIpC (Sigma-Aldrich, St. Louis, MO) every other day for 3 injections. Mice were analyzed starting 2 months after pIpC induction.

CD41 magnetic cell separation of megakaryocytes

Cells were stained with a fluorescein isothiocyanate (FITC) anti-mouse CD41 and then magnetically labeled with anti-FITC MicroBeads (Miltenyi Biotec, Auburn, CA). The cell suspension was loaded on a magnetic-activated cell sorting column placed in the magnetic field of a magnetic-activated cell sorting separator. The magnetically retained cells were eluted as the positively selected cell fraction. Samples were analyzed on a BD FACSCalibur flow cytometer (Becton Dickinson). Acquisition and data analysis were performed using CellQuest Pro software (Becton Dickinson). CD41$^+$ cells purity was >90%.

qRT-PCR analysis

RNA was extracted with Trizol reagent and reverse-transcribed with RT-kit plus (Nanogene). Quantitative reverse transcriptase-PCR (qRT-PCR) was performed using SYBR Green PCR MasterMix and a 7900 Fast Real-Time PCR System (Applied Biosystems, Foster City, CA). PCR amplifications were performed by incubation at 95°C for 10 minutes, followed by 40 cycles of incubations at 95°C for 15 seconds and 60°C for 1 minute. Data were analyzed according to the comparative Ct method and normalized to glyceraldehyde-3-phosphate dehydrogenase expression levels within each sample. The $2^{-\Delta\Delta Ct}$ method was used to calculate relative expression levels of target genes. Data analysis was performed using the SDS Enterprise Database (Applied Biosystems).

miRNA RT-PCR

Real-time PCR for mature *miR-10a* (Assay ID 000387), *miR-10b* (Assay ID 000388), and *miR-20a* (Assay ID 000580), and immature *miR-10a* (Assay ID Mm03307058_pri), *miR-10b* (Assay ID Mm03306401_pri), and *miR-20a* (Assay ID Mm03307063_pri) was performed using a standard TaqMan PCR kit protocol (Applied Biosystems). The reactions were incubated at 95°C for 10 minutes, followed by 40 cycles of 95°C for 15 seconds and 60°C for 1 minute. miRNA expression data were normalized to snoRNA202 (Assay ID 001232).

Immunoblotting analysis

NPM1 mutant protein was detected on lysates from 1 to 2 × 10^6 cells by western blot analysis with a rabbit polyclonal antibody against the mutated NPM1 protein.[29] Lysates from the OCI/AML3 cell line, expressing the NPM1 mutant A protein,[30] were used as control. A monoclonal anti-NPM1 antibody (Zymed) was used to recognize the endogenous mouse Npm1. Nuclear and cytoplasmic extracts were made using the Nuclear Extract Popper kit (Pierce).

Murine peripheral blood counts

Mice were anesthetized with isoflurane followed by retro-orbital bleeding. Blood was taken into glass capillary tubes. Complete blood count was performed using an XE-2100 hematology automated analyzer (Dasit).

Flow cytometry

Flow cytometric analysis was performed on bone marrow (BM) cells and splenocytes using the following monoclonal antibodies: biotin-conjugated antibodies against CD3, CD4, CD8, B220, Ter119, Mac-1, Gr-1, Sca-1, IL7R, CD5, phycoerythrin (PE)-Cy5–conjugated streptavidin, allophycocyanin-eFluor-780–conjugated anti–c-Kit, FITC-conjugated anti-CD41, FITC-conjugated anti–Ly-6A/E(Sca-1), anti-CD135 (eBioscience), allophycocyanin-conjugated anti-CD150, PE/CY7-conjugated anti-CD105 (BioLegend), and PE-conjugated anti-CD16/32 (BD Biosciences). Megakaryocytic progenitors (MKPs) were gated as Lin$^-$c-Kit$^+$Sca-1$^-$CD150$^+$CD41$^+$ cells, and erythromegakaryocytic progenitor cells (Pre-MegE) were gated as Lin$^-$c-Kit$^+$Sca-1$^-$CD41$^-$CD105$^-$CD150$^+$ cells.[31] Cell acquisition and analysis were performed on either a Cytomics FC500 cytometer equipped with the CXP analysis software 2.0 (Beckman Coulter) or a FACSCanto flow cytometer using the FACSDiva software (BD Biosciences). Gates were drawn to exclude nonviable cells and debris. Part of the flow cytometry data was analyzed with FlowJo software (Tree Star, Ashland, OR).

In vitro hematopoietic colony-forming assay

For MegaCult-C assays, a total of 10^5 BM mononuclear cells were used according to the manufacturer's protocols (Stem-Cell Technologies, Vancouver, Canada); 50 ng/mL human thrombopoietin (TPO), 50 ng/mL human interleukin (IL)-11, 10 ng/mL murine IL-3, and 20 ng/mL human IL-6 (PeproTech, Rocky Hill, NJ) were used in these assays. The cultures were incubated at 37°C with 5% CO_2 for 6 to 8 days. Colonies containing >3 megakaryocytes (AchE$^+$ cells) were considered colony forming unit-megakaryocytes (CFU-MKs). Duplicate assays were performed for each mouse.

Serum TPO concentration measurement

The Quantikine murine TPO immunoassay kit (R&D Systems, Minneapolis, MN) was used to quantify TPO concentration in harvested sera.

Megakaryocytes in BM biopsies from *NPM1*-mutated AML patients

The number of megakaryocytes was assessed by immunohistochemistry in BM biopsies from 97 patients with *NPM1*-mutated AML. BM biopsies from 10 lymphoma patients that turned out to be normal at histologic examination were used as controls. Megakaryocytes labeling was performed in paraffin sections using a mouse monoclonal antibody against the linker for activation of

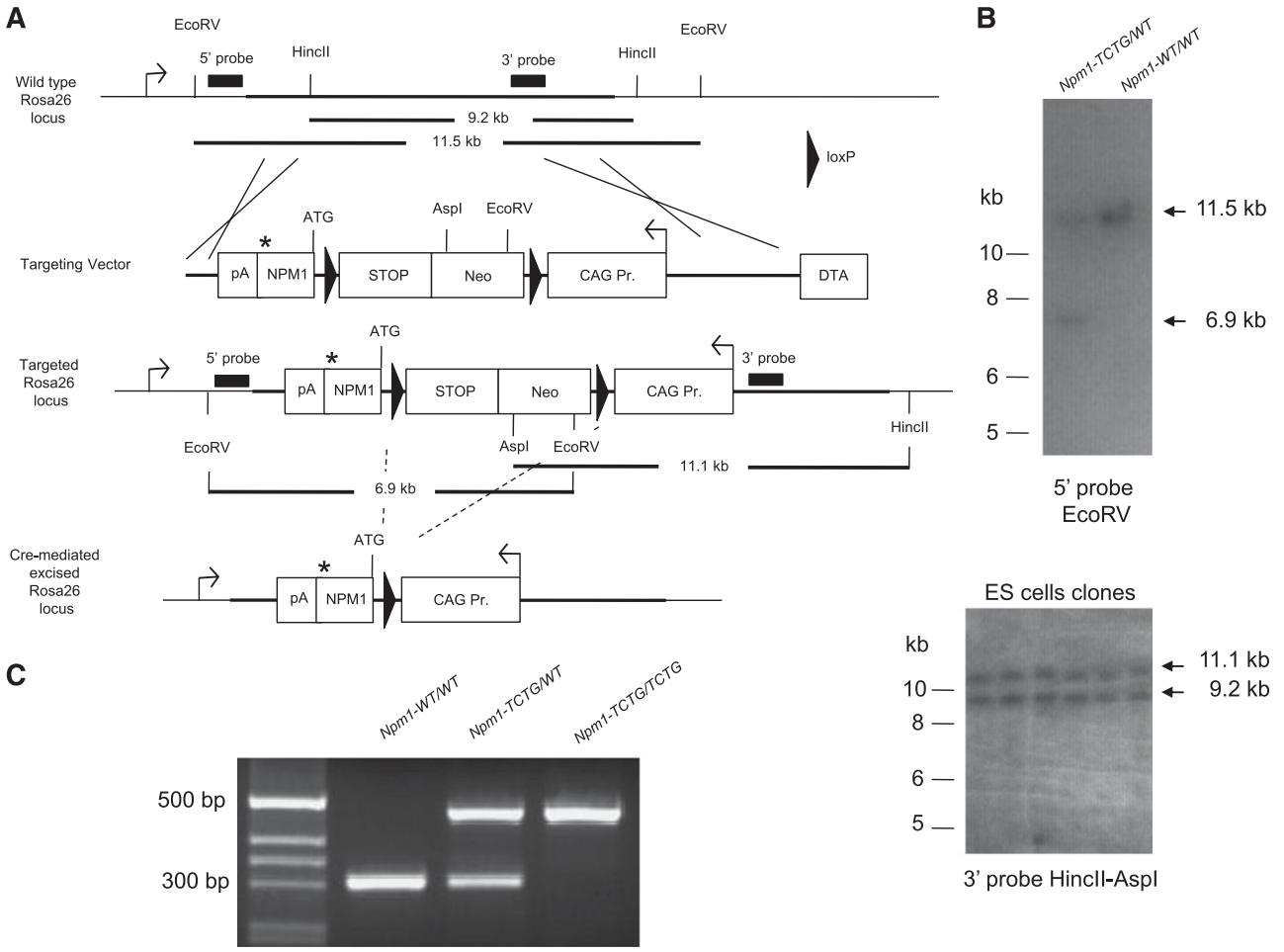

Figure 1. Generation of a conditional mouse model with the human *NPM1* mutation A. (A) Strategy for targeted insertion of a human *NPM1* mutation A cDNA into the murine ROSA26 genomic DNA locus. The figure describes the structure of the mouse ROSA26 locus (top), the targeting vector (upper middle), the targeted allele (lower middle), and Cre-mediated excised allele (bottom). The targeting vector was a 16-kb plasmid containing a transgenic cassette expressing the *NPM1* mutant cDNA (NPM1; *position of the TCTG duplication), a combined loxP flanked STOP-Neomycin selection cassette, an inducible CAG promoter, and a negative DTA selection marker. *NEO* is excised through Cre-mediated recombination between the 2 lox*P* sites (triangles). Positions of the 5′ and 3′ probes used to confirm the homologous recombination and relevant restriction sites for Southern blot analysis are indicated. (B) Southern blotting analysis confirmed the presence of homologous recombination in Npm1-TCTG/WT mice (top) and ES cells (bottom). (C) PCR genotyping strategy for Npm-TCTG/WT mice to distinguish the wild-type allele (304 bp) from the knocked-in recombined allele (472 bp).

T cells (LAT) protein (Dako) that is an excellent marker for megakaryocytes in BM biopsies.[32] Care was taken to exclude from the count activated T cells that were distinguishable from megakaryocytes because of their weaker LAT positivity and different morphology. The antibody-antigen reaction was detected by an immuno-alkaline phosphatase procedure.[19] The adjusted megakaryocytes concentration was determined by 2 independent investigators (PS and BF) with the following formula: (measured megakaryocytes concentration × 100)/percent cellularity.[33] Histopathology images were acquired with the ×40/0.85 and ×4/0.16 objectives (Olympus U Plan Apo) of an Olympus BX61 microscope equipped with an Olympus DP71 digital camera, using the Olympus cell^B acquisition software.

Statistical analysis

The statistical significance of differences between different conditions was determined using Prism (GraphPad Software, La Jolla, CA) with a 2-tailed unpaired *t* test.

Results

Generation of conditional mice for the human *NPM1* mutation A

We generated a novel *NPM1* mutation mouse model by targeted insertion of the human *NPM1* mutation A cDNA into the *Rosa26* locus via homologous recombination in embryonic stem (ES) cells (Figure 1A). The targeting vector includes a combined STOP-neomycin selection cassette flanked by two *lox*P sites that can be removed on Cre induction, allowing for the expression of the *NPM1* mutant under the control of a CAG promoter.

ES cells that had undergone homologous recombination, as determined by Southern blot analysis (Figure 1B), were microinjected into C57BL/6J blastocysts to generate chimeric mice. Following germ-line transmission from chimeric mice, the resulting heterozygous progeny (*Npm1-TCTG/WT*) was intercrossed and analyzed by Southern blot to confirm correct targeting of the transgene at the *ROSA26* locus (Figure 1B). *Npm1-TCTG/WT* mice were viable and fertile, exhibited normal survival, and manifested no gross phenotypic abnormalities.

To study the effects of the *NPM1* mutation in the hematopoietic compartment, the *Npm1-TCTG/WT* mice were crossed with transgenic *Mx1-Cre* mice. The *Mx1* promoter was activated by pIpC treatment,[34] leading to Cre expression in hematopoietic cells. Cre-mediated excision of the STOP-neomycin selection cassette was detectable in BM cells starting 1 month after pIpC induction (supplemental Figure 1). The offspring of *Npm1-TCTG/WT;Cre*$^+$ crosses were born at Mendelian ratios.

Cre-dependent expression of *NPM1* mutation in the hematopoietic compartment

We next sought to verify that *NPM1* mutation A transgene expression could be induced in a Cre-dependent manner. For this purpose, we treated 6- to 12-week-old *Npm1-TCTG/WT;Cre*$^+$ and *Npm1-TCTG/WT;Cre*$^-$ with pIpC and analyzed the mice 8 weeks later. The expression of the *NPM1* mutation A mRNA was detected in BM cells (Figure 2A), spleen, and peripheral blood by quantitative real-time PCR using primers specific for the human *NPM1* mutant.[35] Moreover, we monitored transgene expression in peripheral blood samples, demonstrating that the *NPM1* mutant mRNA levels were stable up to 24-month follow-up. Using an antibody specific for the NPM1 mutant,[29] we confirmed that the mutant protein was present in *Npm1-TCTG/WT;Cre*$^+$ mice in different hematopoietic tissues (Figure 2B). *Npm1-TCTG/TCTG;Cre*$^+$ mice expressed approximately twofold higher mutant protein levels in BM cells compared with heterozygous Cre$^+$ mice (Figure 2C) and a band intensity similar to the endogenous Npm1. Additional western blot analysis demonstrated the expression of the mutant protein in CD41$^+$ megakaryocytic, Gr-1$^+$ myeloid, and CD3/B220$^+$ T- and B-lymphoid cells in the BM of *Npm1-TCTG/WT;Cre*$^+$ mice (Figure 2D). Myeloid cells showed higher levels of the NPM1 mutant compared with the endogenous Npm1 protein, whereas CD41$^+$ cells displayed an equal mutant/wild-type ratio. Nevertheless, no conclusions can be made about the absolute ratio of endogenous vs mutant NPM1 proteins, because different antibodies were used in western blotting experiments.

Finally, we looked at NPMc$^+$ expression in mutant mice compared with blasts from 3 NPMc$^+$ AML patients, and we found that NPMc$^+$ protein levels in the homozygous mice paralleled those of NPMc$^+$ in human AML (Figure 2E). Therefore, our data show that expression of NPM1 mutant protein in BM cells and isolated hematopoietic cells is comparable to that of WT protein encoded by the endogenous locus and increases in a dose-dependent fashion in *Npm1-TCTG/TCTG;Cre*$^+$.

Nucleophosmin dislocation into cytoplasm is a functional consequence of *NPM1* mutation in human AML and appears to be a critical leukemogenic event.[18] Evidence of cytoplasmic nucleophosmin in BM cells including megakaryocytes could not be obtained by immunohistochemistry because of the cross-reactivity of the anti-human NPM antibodies with mice tissues. In particular, nonspecific cytoplasmic positivity of megakaryocytes was observed with these antibodies both in control and mutant mice. Thus, we performed western blot analysis on nuclear and cytoplasmic fractions lysates that clearly showed the accumulation of the NPM1 mutant in the cytoplasm of BM cells from *Npm1-TCTG/WT;Cre*$^+$ mice (Figure 2F).

Platelet numbers are markedly reduced in *Npm1-TCTG/WT;Cre*$^+$ mice

After pIpC treatment, complete peripheral blood counts were monitored in *Npm1-TCTG/WT;Cre*$^+$ and age-matched *Npm1-TCTG/WT;Cre*$^-$ littermate controls for 18 months. Strikingly, mice expressing the *NPM1* mutation A showed a fully penetrant phenotype in the peripheral blood, characterized by significantly lower platelet counts compared with *Npm1-TCTG/WT;Cre*$^-$ pIpC-treated controls (Figure 3A). Platelets were one-half of the control count in mutants harboring 1 conditional allele and one-quarter in homozygous *Npm1-TCTG/TCTG;Cre*$^+$ mice ($P < .001$; Figure 3B). Moreover, the few circulating platelets were considerably larger than normal in mutant mice as shown by the increased mean platelet volume (8.07 ± 0.39 vs 6.250 ± 0.13 femtoliter; n = 4, $P < .01$; Figure 3Ci). *Npm1-TCTG/WT;Cre*$^+$ also displayed increased platelet distribution width (8.55 ± 0.98 vs 5.25 ± 0.11 femtoliter; n = 4, $P < .05$) and platelet-large cell ratio (15.18 ± 2.88% vs 2.42 ± 1.06%; n = 4, $P < .01$) compared with *Npm1-TCTG/WT;Cre*$^-$ mice (Figure 3Cii-iii). Peripheral blood smears confirmed both the paucity of platelets in *Npm1-TCTG/WT;Cre*$^+$ relative to littermate *Cre*$^-$ controls and their substantially larger size (Figure 3Civ). Mutant mice showed a tendency to prolonged bleeding times (supplemental Figure 2). Complete blood count analysis revealed no significant changes in white blood cell counts and hemoglobin levels (Figure 3A; supplemental Table 1). Almost all the animals survived to 1.5 years of age without gross evidence of disease.

Megakaryocytes expansion and block of differentiation in *Npm1-TCTG/WT;Cre*$^+$ mice

To investigate whether the reduced platelet number in the *Npm1-TCTG/WT;Cre*$^+$ mice might result from abnormal hematopoiesis, we performed flow cytometric analysis of BM cells. For this purpose, we used CD41 as a marker that is expressed throughout megakaryocyte differentiation from early progenitors to mature megakaryocytes and platelets.[36] Interestingly, there was a significant increase of more than twofold in the percentage of CD41$^+$ cells in *Npm1-TCTG/WT;Cre*$^+$ BM and close to fourfold in *Npm1-TCTG/TCTG;Cre*$^+$ samples compared with control mice (5.28 ± 3.57% vs 7.94 ± 2.4% vs 2.52 ± 1.4%, respectively; Figure 4A-B). This difference remained significant after adjusting for BM cellularity, which was similar along the 3 groups (Figure 4C). CD41$^+$ cells also accumulated in the spleen of *Npm1-TCTG/WT;Cre*$^+$ and *Npm1-TCTG/TCTG;Cre*$^+$ mice, most likely as a result of extramedullary hematopoiesis contributing to a mild splenomegaly (Figure 4D-E). Interestingly, serum TPO levels did not differ between heterozygous, homozygous mutants, and control mice (Figure 4F). Altogether, these findings suggest that the expression of the NPM1 mutant determines a block of megakaryocytes differentiation rather than an increased number of megakaryocytes secondary to platelets destruction.

To further characterize the megakaryocytic compartment in mutant mice, we assessed the presence of early MKPs cells in the BM. Lin$^-$ Kit$^+$Sca-1$^-$CD150$^+$CD41$^+$ MKP cells were increased twofold in *Npm1-TCTG/WT;Cre*$^+$ mice and up to fourfold in *Npm1-TCTG/TCTG;Cre*$^+$ compared with *Cre*$^-$ controls (0.15 ± 0.07% vs 0.24 ± 0.15% vs 0.05 ± 0.02%, respectively; Figure 5A-B), suggesting that *NPM1* mutant A expression drives the expansion of immature megakaryocytes. There was no significant difference in the percentage of Lin$^-$Kit$^+$Sca-1$^+$ (LSK) cells and pre-MegE cells in the BM of the 3 animal groups (Figure 5C). To better characterize the perturbation in megakaryocyte growth, we subsequently conducted in vitro colony-forming assays. Interestingly, *Npm1-TCTG/WT;Cre*$^+$ BM cells formed significantly more megakaryocytic colonies (CFU-MK) than *Cre*$^-$ control in semisolid media (34.00 ± 5.367 vs 9.0 ± 1.265 CFU-MK/10^5 BM cells; n = 6, $P < .01$; Figure 5E), whereas CFU-MK sizes were similar (Figure 5F).

Overall, our findings strongly suggest the *NPM1* mutant blocks the differentiation of megakaryocytes with a consequent decrease in production of mature platelets (Figure 5G).

Features of myeloproliferation in *Npm1-TCTG/WT;Cre*$^+$ mice

Flow cytometric and additional pathological analysis revealed that ~15% of *Npm1-TCTG/WT;Cre*$^+$ mice displayed features of myeloproliferation in the BM and spleen. In particular, BM samples from *Npm1-TCTG/WT;Cre*$^+$ mice showed an increased number of mature Gr1$^+$Mac1$^+$ myeloid cells and decreased number of B220 B cells compared with *Cre*$^-$ control mice (84.31 ± 7.55% vs 55.24 ± 14.75% and 4.35 ± 3.62% vs 19.86 ± 6.18%, respectively;

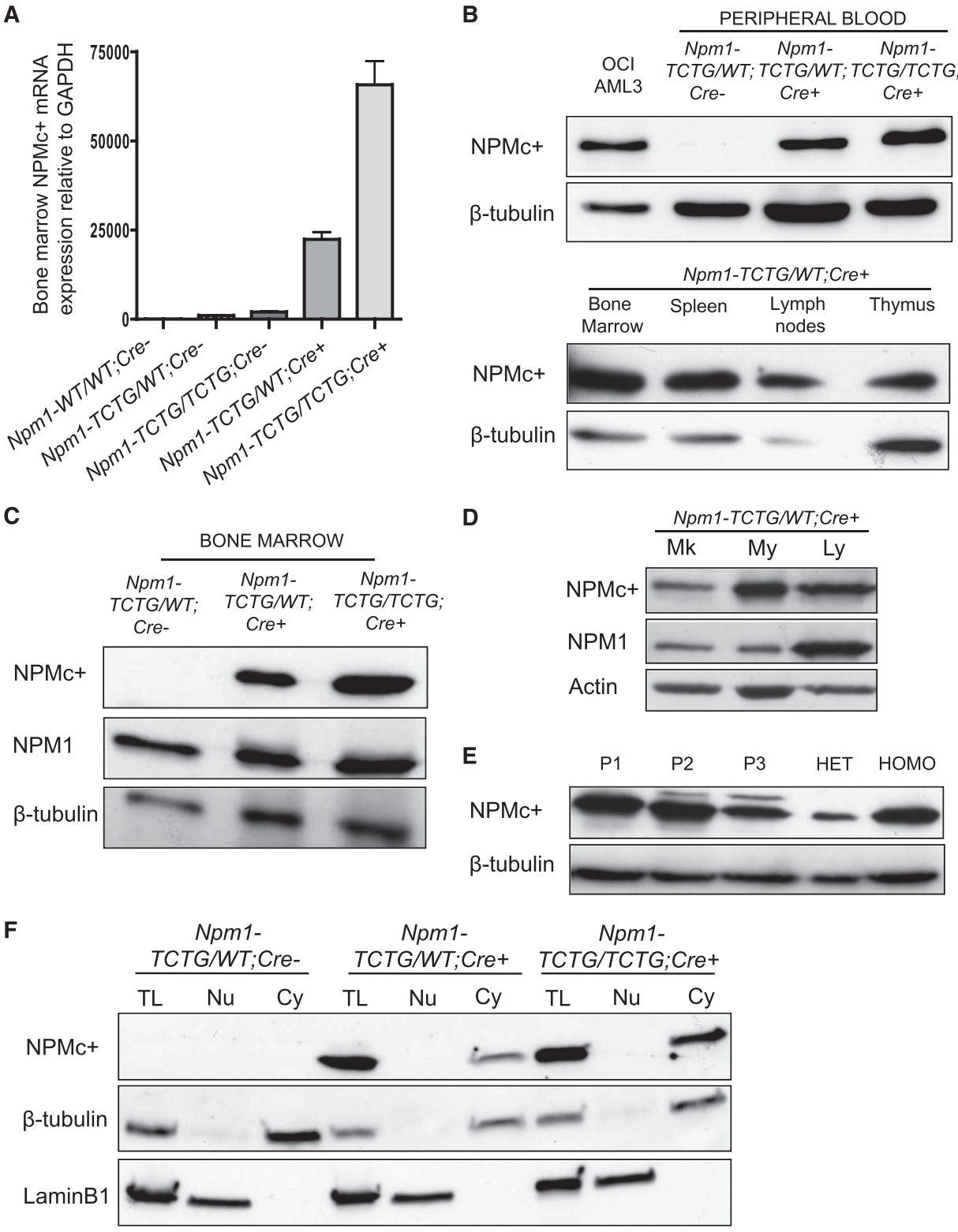

Figure 2. Expression levels of the NPM1 mutation A in mouse hematopoietic tissues. (A) RT-PCR detected transcription of the NPM1 mutant (NPMc$^+$) mRNA in the BM of mutant mice 2 months after pIpC induction of the Cre. (B) Expression of the NPM1 mutant protein in peripheral blood lysates (left) and in hematopoietic tissues (right) using a specific antibody against the mutant. (C) Different expression levels of the NPM1 mutant in BM cells from heterozygous (Npm1-TCTG/WT;Cre$^+$) vs homozygous (Npm1-TCTG/TCTG;Cre$^+$) mice normalized to endogenous Npm1. (D) Western blot of magnetic-activated cell sorting–sorted CD41$^+$ megakaryocytic (Mk), Gr-1$^+$ myeloid (My), and CD3/B220$^+$ T- and B-lymphoid (Ly) cells compared with whole BM of Npm1-TCTG/WT;Cre$^+$ pIpC-induced mice. (E) NPM1 mutant protein expression in 3 different NPM1-mutated AML patients (P1, P2, and P3) compared with heterozygous (HET) and homozygous (HOMO) mutant mice BM. (F) Western blot analysis of NPMc$^+$ expression on nuclear and cytoplasmic fractions of BM cells from heterozygous and homozygous mutant mice. C, cytoplasmic fraction; N, nuclear fraction; TL, total lysate.

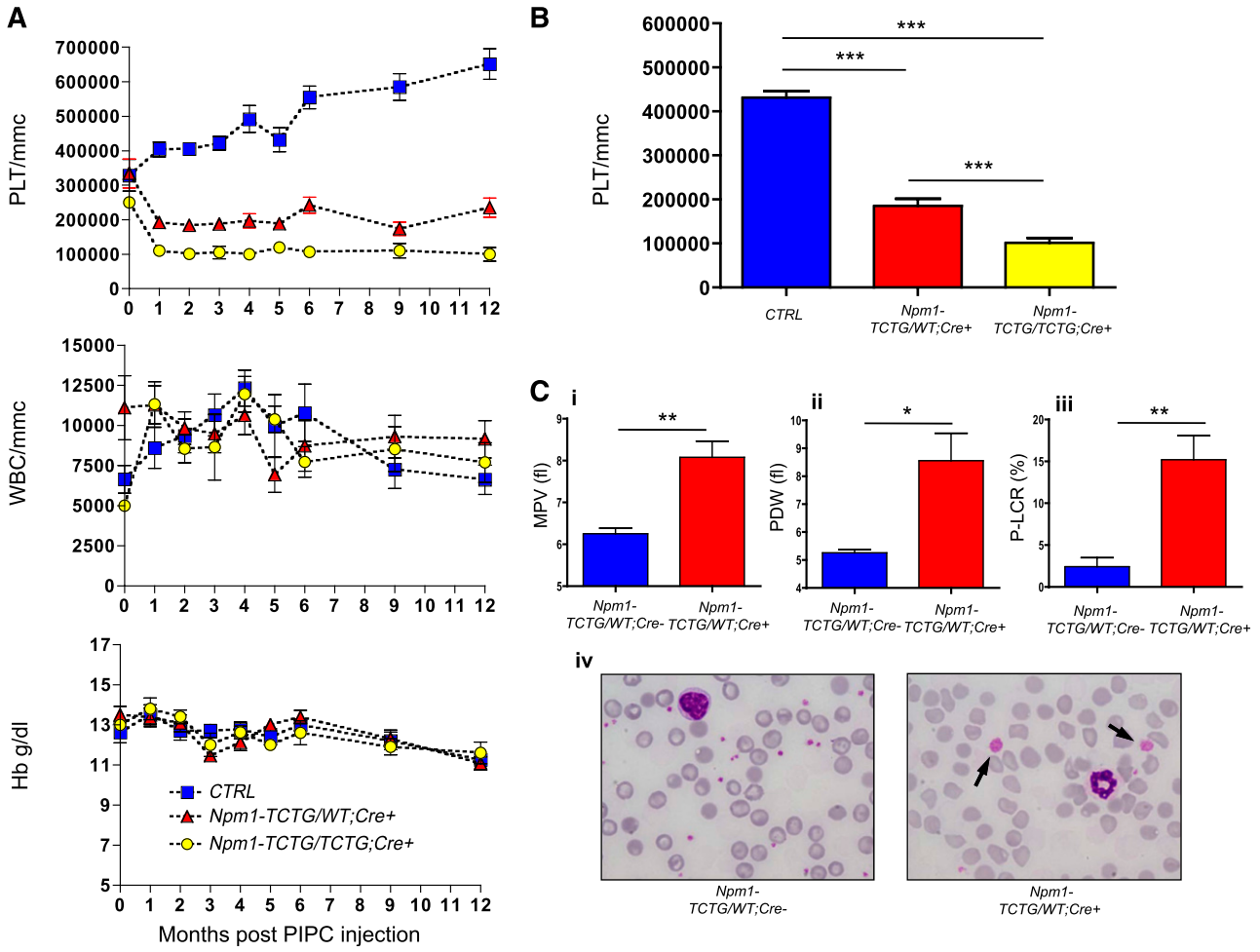

Figure 3. Thrombocytopenia of Cre-induced mice harboring the mutated NPM1 cDNA transgenic cassette. (A) Peripheral blood cell counts of *Npm1-TCTG/WT;Cre*$^{+}$ (n = 9) and *Npm1-TCTG/TCTG;Cre*$^{+}$ (n = 8) vs control mice (n = 9; including 3 *Npm1-WT/WT;Cre*$^{+}$, 3 *Npm1-TCTG/WT;Cre*$^{-}$, and 3 *Npm1-TCTG/TCTG;Cre*$^{-}$ pIpC-treated mice). (B) Significantly decreased platelets number in peripheral blood of both heterozygous and homozygous conditional mice 1 month after pIpC injection. Results are shown as mean ± standard deviation (error bars) from 13 *Npm1-TCTG/WT;Cre*$^{+}$ and 10 *Npm1-TCTG/TCTG;Cre*$^{+}$ vs 25 control mice (including *Npm1-WT/WT;Cre*$^{+}$ [n = 9], *Npm1-TCTG/WT;Cre*$^{-}$ [n = 9], and *Npm1-TCTG/TCTG;Cre*$^{-}$ [n = 7] pIpC-treated mice). (C) Enlarged platelet size in *Npm1-TCTG/WT;Cre*$^{+}$ mice (N = 4) is shown as increased (i) mean platelet volume, (ii) platelet distribution width, and (iii) platelet-large cell ratio. (iv) Peripheral blood smears showing both the paucity of platelets and their substantially larger size (arrows) in heterozygous mutant mice vs littermate Cre^{-} pIpC-treated controls. *$P < .05$, **$P < .01$, ***$P < .001$ (unequal-variance *t* test).

supplemental Figure 3A-B). This was further confirmed by histologic analysis of spleen sections, where expansion of myeloid cells was observed in the red pulp of *Npm1-TCTG/WT;Cre*$^{+}$ mice (supplemental Figure 4), along with an increased megakaryocyte number. In addition, the number of CFU-GM colonies derived from BM cells of *Npm1-TCTG/WT;Cre*$^{+}$ mice showed a trend toward increase compared with Cre^{-} mice that was significant for colonies in *Npm1-TCTG/TCTG;Cre*$^{+}$ mice (Figure 5D). However, histologic analysis of BM sections failed to reveal significant morphologic differences between the mutant and control mice. No age-matched *Npm1-TCTG/WT;Cre*$^{-}$ controls showed signs of disease development. Altogether, these data support evidence of the presence of a myeloid defect in a fraction of NPMc^{+} mutant mice and are consistent with previous reports.[24,26]

Overexpression of *NPM1* mutant induces *miR-10a*, *miR-10b*, and *miR-20a* in vivo

Recent findings suggest a role for miRNAs during megakaryopoiesis where *miR-10a*, *miR-10b,* and *miR-20a* appear to be down-regulated as the cell commits to mature megakaryocytes.[37,38] Hypothetically, the down-regulation of miRNAs unblocks the expression of target genes involved in megakaryocyte differentiation. Thus, we analyzed whether the expression of *miR-10a*, *miR-10b,* and *miR-20a* was altered in our mutant mice. Strikingly, both heterozygous and homozygous Cre^{+} mutant mice displayed significant miRNAs overexpression compared with Cre^{-} controls. The expression of *miR-10*a, *miR-10b* and *miR-20a* in CD41^{+} cells from *Npm1-TCTG/WT;Cre*$^{+}$ vs *Npm1-TCTG/TCTG;Cre*$^{+}$ mice increased 1.96-, 2.15-, and 1.69-fold vs 4.36-, 5.96-, and 2.88-fold respectively, compared to *Npm1-TCTG/WT;Cre*$^{-}$ mice (Figure 6A).

To demonstrate that altered miRNAs expression was directly related to NPM1 shuttling dysfunction, we measured immature to mature miRNAs ratios in *Npm1-TCTG/WT;Cre*$^{+}$ mice compared with Cre^{-} controls. The NPM1 mutant is associated with a significant reduction of the immature to mature miR-10a and miR10b ratio because of a decrease in miRNA precursors coupled with a concomitant increase in mature miRNA level (supplemental Figure 5). Moreover, miR10a, 10b, and 20a levels significantly increased 1.55-, 3.07-, and 1.27-fold, respectively, in NIH-3T3 cells overexpressing

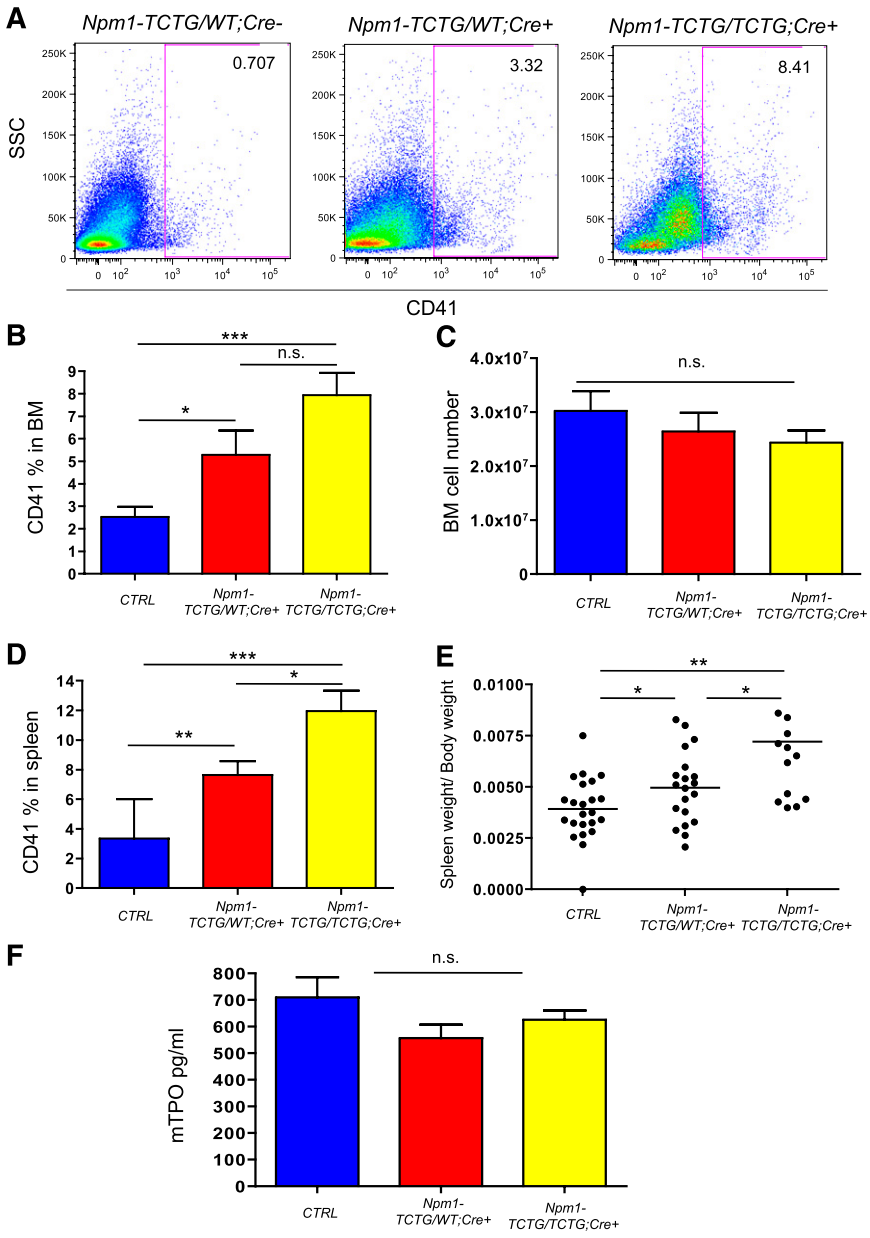

Figure 4. Expansion of the CD41$^+$ megakaryocytes in *Npm1-TCTG/WT;Cre*$^+$ and *Npm1-TCTG/TCTG;Cre*$^+$ mice. (A) Flow cytometric analysis of single-cell suspensions of BM from representative *Npm1-TCTG/WT;Cre*$^+$, *Npm1-TCTG/TCTG;Cre*$^+$, and *Npm1-TCTG/WT;Cre*$^-$ pIpC-treated control mice demonstrates an increase in the percentage of CD41$^+$ megakaryocytic cells. (B) Quantification of CD41$^+$ megakaryocytic cells in the BM of age-matched mutant mice analyzed as in panel A: *Npm1-TCTG/WT;Cre*$^+$ (n = 11) and *Npm1-TCTG/TCTG;Cre*$^+$ (n = 6); *CTRL* indicates control mice including *Npm1-WT/WT;Cre*$^+$ (n = 3), *Npm1-TCTG/WT;Cre*$^-$ (n = 7), and *Npm1-TCTG/TCTG;Cre*$^-$ (n = 2) pIpC-treated mice. (C) BM cellularity in *Npm1-TCTG/WT;Cre*$^+$ (n = 11), *Npm1-TCTG/TCTG;Cre*$^+$ (n = 6), and control mice (genotypes and numbers are the same as in panel B). (D) Percentage of CD41$^+$ megakaryocytic cells in the spleen of heterozygous (n = 10) and homozygous (n = 6) mutant mice compared with pIpc-treated Cre$^-$ controls (n = 6). (E) Composite data from age-matched littermates of indicated genotypes demonstrating mild hypersplenism in *Npm1-TCTG/WT;Cre*$^+$ and *Npm1-TCTG/TCTG;Cre*$^+$ mice. (F) Comparison of serum TPO concentration between Cre$^-$ pIpC control mice, *Npm1-TCTG/WT;Cre*$^+$, and *Npm1-TCTG/TCTG;Cre*$^+$ (n = 12 per genotype). $^*P < .05$, $^{**}P < .01$, $^{***}P < .001$ (unequal-variance *t* test). n.s. = not statistically significant.

the NPM1 cDNA mutant (supplemental Figure 6), suggesting that mutant NPM1 expression itself causes an increased miRNA level, which is not simply a consequence of immature megakaryocytes expansion.

It has been reported that in mouse embryonic development, *miR-10a* and *miR-10b* expression closely follows the expression of *Hox* genes in whose cluster they are embedded (*miR-10a* is located between the *HOXB4* and *HOXB5* gene in chromosome 17q21 and *miR-10b* between the *HOXD3* and *HOXD4* gene in chromosome 2q31).[39] To investigate whether *miR-10a* levels correlated with the expression of its flanking *HOXB4* and *HOXB5* genes, we measured their expression in CD41$^+$ cells by qRT-PCR. Notably, CD41$^+$ cells displayed a significant up-regulation of both *HOXB4* and *HOXB5* genes in *Npm1-TCTG/WT;Cre*$^+$ and *Npm1-TCTG/TCTG;Cre*$^+$ mice compared with Cre$^-$ controls (1.68 ± 0.5 vs 4.12 ± 0.23 vs 1.02 ± 0.15 and 1.73 ± 1.16 vs 4.71 ± 4.79 vs 1.00 ± 0.12, respectively; Figure 6B). No correlation was found between *miR-10b* and its flanking *HOXD3* gene.

BM megakaryocytic expansion in *NPM1*-mutated AML

To assess whether alterations of the megakaryocytic compartment similar to those observed in our mouse model were detected also in human AML, we reviewed the characteristics of megakaryocytes in BM biopsies from 97 *NPM1*-mutated AML patients compared with 25 *NPM1*-unmutated AML and 10 nonleukemic BM samples used as controls. The average megakaryocytic concentration in nonleukemic samples was 8.58 ± 1.86 per ×40 field.

BM samples from *NPM1*-mutated AML showed an increased number of megakaryocytes (average megakaryocytic concentration per ×40 field: 13.7 ± 13.2). In particular, the LAT-positive megakaryocyte concentration per ×40 field in the 97 *NPM1*-mutated samples was as follows: <10 in 52/97 (53.6%) cases, >10 in 15/97 (15.4%) cases, >20 in 24/97 (24.7%) cases, and >40 in 6/97 (6.2%) cases (supplemental Table 2).

In contrast, the average megakaryocytic concentration in *NPM1*-unmutated AML samples was 7.6 ± 13.6 per ×40 field.

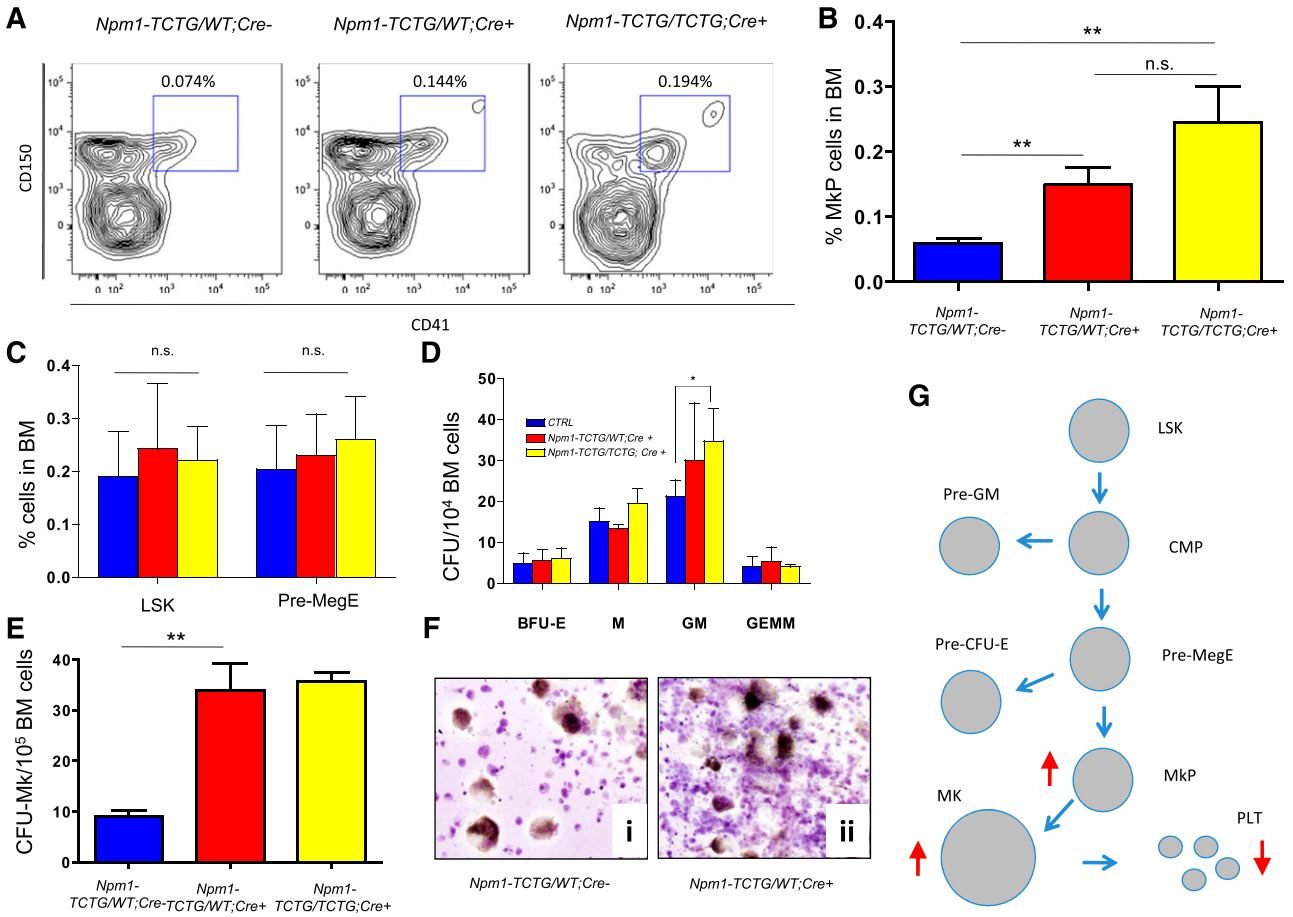

Figure 5. Expansion of the immature megakariocytes in *Npm1-TCTG/WT;Cre*$^+$ and *Npm1-TCTG/TCTG;Cre*$^+$ mice. (A) Flow cytometric analysis of single-cell suspensions of BM from representative *Npm1-TCTG/WT;Cre*$^+$, *Npm1-TCTG/TCTG;Cre*$^+$, and *Npm1-TCTG/WT;Cre*$^-$ pIpc-treated control mice demonstrates an increase in the percentage of Lin$^-$Kit$^+$Sca-1$^-$CD150$^+$CD41$^+$ megakaryocytic progenitor populations. (B) Quantification of Lin$^-$Kit$^+$Sca-1$^-$CD150$^+$CD41$^+$ MKPs in the BM of age-matched mutant mice analyzed as in panel A (n = 8 per genotype). (C) No differences in the percentage of Lin$^-$Kit$^+$Sca-1$^+$ cells and Lin$^-$Kit$^+$Sca-1$^-$CD41$^-$CD150$^+$FcgR$^-$CD105^{lo} erythromegakaryocytic progenitor cells in mutant Cre$^+$ vs Cre$^-$ pIpC-treated control mice (n = 6 per genotype). (D) BM cells from *Npm1-TCTG/WT;Cre*$^+$, *Npm1-TCTG/TCTG;Cre*$^+$, and *Cre*$^-$ pIpC-treated mice were plated on M3434 methylcellulose medium (containing stem cell factor, IL-3, IL-6, erythropoietin) and scored for colony formation 7 to 10 days later (BFU-E, burst-forming unit-erythroid; GEMM, granulocyte, erythroid, monocyte, megakaryocyte; GM, granulocyte monocyte; M, monocyte). Results are the average of 3 independent experiments performed in duplicate (mean ± standard deviation are shown). (E) CFU-MK potential from total BM (n = 3 per genotype). (F) Photo of representative colonies (×10 magnification) from (ii) *Npm1-TCTG/WT;Cre*$^+$ compared with (i) *Npm1-TCTG/WT;Cre*$^-$. (G) Summary of the alterations in the development of the megakaryocytes after the expression of the NPM mutation A in the hematopoietic compartment. $^{**}P < .01$; n.s. = not statistically significant.

In particular, only 16% (4/25) of *NPM1*-unmutated AML patients showed an average megakaryocyte concentration >10. Overall, our data indicated that the percentage of BM samples with megakaryocytosis is increased to 46.4% in *NPM1*-mutated AML compared with 16% of *NPM1*-unmutated AML samples. BM samples with a megakaryocytic concentration <10 were more in the *NPM1*-unmutated than in the *NPM1*-mutated AML group (84% vs 53.6%, respectively).

Immunohistochemistry usually resulted in a higher scoring of the number of megakaryocytes than histologic examination, because it allowed better detection of dysplastic megakaryocytes and micromegakaryocytes (Figure 7). At immunostaining, most of the megakaryocytes were characterized by cytoplasmic positivity for NPM and nuclear-restricted expression for nucleolin/C23, clearly indicating that they carried the *NPM1* mutation. Among the 45 cases with an increased megakaryocyte concentration, 38 presented with thrombocytopenia, 6 cases with a normal number of platelets, and only 1 case with thrombocytosis. Thus, the expansion of megakaryocytic compartment in human *NPM1*-mutated AML patients mimics that observed in our NPMc$^+$ mice model.

Discussion

In this study, we generated and characterized a new mouse model expressing the most frequent human *NPM1* mutation (type A) in the hematopoietic stem cell compartment to investigate the role of the NPM1 mutation in leukemogenesis. Similarly to other animal models for *NPM1* mutation,[24-26] we found an expansion of the myeloid compartment in a fraction of mice. In addition, we demonstrated for the first time that the NPM1 mutant leads to perturbation of the megakaryocytic compartment in mice. This phenotype mimics some of the features observed in patients with *NPM1*-mutated AML.

Our observation that megakaryocytes from *Npm1-TCTG/WT;Cre*$^+$ mice exhibit deregulated growth in vitro and in vivo points to a role of the NPM1 mutant in megakaryocytic differentiation. Mice expressing the NPM1 mutant have decreased platelet counts with a markedly increased mean platelet volume. There is also a remarkable megakaryocytosis in these animals, with a significant increase in megakaryocyte numbers both in BM and spleen. Megakaryocytosis is driven by an increased number of CFU-Meg and a pronounced

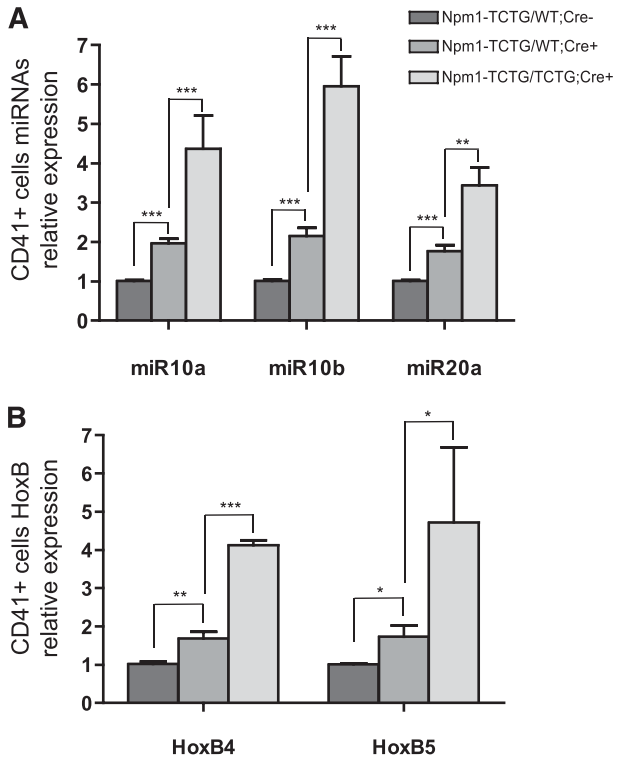

Figure 6. *miR-10a, miR10b*, and *miR20a* overexpression correlates with *HOXB* gene expression. (A) miRNA qRT-PCR for *miR-10a, miR-10b,* and *miR-20a* in CD41$^+$ cells from *Npm1-TCTG/WT;Cre*$^+$ and *Npm1-TCTG/TCTG;Cre*$^+$ mice vs Cre$^-$ controls. (B) Relative gene expression of *HoxB4* and *HoxB5* in the BM of *Npm1-TCTG/WT;Cre*$^+$ and *Npm1-TCTG/TCTG;Cre*$^+$ mice vs Cre$^-$ controls. qRT-PCR was performed on pooled CD41$^+$ magnetic-activated cell sorting–sorted cells from ≥3 mice per genotype. Histograms represent mean miRNA expression from triplicate samples obtained from 3 independent experiments. $^*P < .05$, $^{**}P < .01$, $^{***}P < .001$ (unequal-variance *t* test).

expansion of early MKP cells that is not accompanied by altered TPO levels. CD41$^+$ megakaryocytes display altered expression of miRNAs directly involved in human and mouse megakaryopoiesis. These findings suggest that the NPM1 mutant is able to induce a block of megakaryocytic differentiation, although we cannot exclude the possibility of a partial contribution on regulating platelet budding.

Notably, the effects of the NPM1 mutant on megakaryopoiesis that we observed in our model was not previously reported by other investigators.[26,40] Because cytoplasmic localization of the NPM1 mutant appears to be critical for the development of *NPM1*-mutated AML,[18] it is likely that these conflicting results may be caused by differences in the degree of the relative dosage of the mutated vs normal NPM1 and consequent alterations in the distribution of these proteins across subcellular compartments among different models. In our mice, the transgenic cassette that was used to express the NPM1 mutant cDNA under the control of a CAG promoter may have driven the expression of the NPM1 mutant to an extent to influence the mutated vs normal *NPM1* ratio, thus leading to conditions pathophysiologically mimicking more closely those of human *NPM1*-mutated AML. In contrast, in the first transgenic NPMc$^+$ model,[24] the degree of the expression of NPM1 mutant was not as high as that of wild-type NPM1, determining a mild cytoplasmic expression and a nuclear relocalization of the mutant, as it can be simulated in vitro by cotransfection experiments.[20] Moreover, in the conditional knock-in mouse model reported by Vassiliou et al,[26] the cytoplasmic accumulation of the mutant NPM1 was not clearly shown in BM cells from mutant animals because only total cell lysates were analyzed for the mutant expression. Nevertheless, the same study also described an increase of the mean platelet volume similar to our model, even though blood counts and platelet numbers were not altered in mutant mice.[26] Finally, the observation that in our *NPM1* homozygous mutant mice platelet counts were further decreased to a half of the heterozygous mice further reinforces the concept that the NPM1 mutant is likely to exert its function and alter platelets formation depending of the mutant to wild-type NPM1 ratio.

The expression of *NPM1* mutation in the hematopoietic compartment promoted by the inducible *Mx1Cre* caused the overexpression of *miR10a*, *miR10b,* and *miR-20a* in CD41$^+$ cells. The relevance of this finding is related to the fact that miRNAs are expressed in megakaryocytes and platelets, where they are likely to regulate lineage development and function. Garzon et al[37] showed that differentiation of human CD34$^+$ cells into megakaryocytes is accompanied by down-regulation of numerous miRNAs including *miR10a* and *miR10b*. Other investigators found the expression of *miR-20a* to be reduced more than twofold in mature megakaryocytes compared with hematopoietic progenitors.[38] Moreover, *miR10a*, *miR10b,* and *miR-20a* appear to be directly involved in megakaryocytic development by posttranscriptional inhibition of targeted genes expression that allow megakaryocytic precursors to produce platelets.[37] Thus, the NPM1 mutant–related increased expression in *miR10a*, *miR10b,* and *miR-20a* may be responsible for the block of differentiation of megakaryocytes in our mouse model. This view is further supported by previous reports showing that the 3 up-regulated miRNAs in our mouse model also contribute to define the distinct microRNA profile of *NPM1*-mutated AML patients.[7,10] The interference of the NPM1 mutant with the megakaryocytic compartment is also consistent with clinico-pathological observations that BM biopsies from a significant number of patients with *NPM1*-mutated AML show myelodysplastic features affecting ⩾2 hemopoietic progenitors, especially megakaryocytes.[41,42] In this paper, we further expanded these findings with a more accurate quantitative evaluation of megakaryocytes by immunohistochemistry with the anti-LAT antibody. Notably, we found an increased number of megakaryocytes in *NPM1*-mutated AML compared with *NPM1*-unmutated AML and normal controls. These findings are in keeping with the expansion of the megakaryocyte compartment observed in our NPM1c$^+$ mouse model.

Although the mechanism underlying the up-regulation of *miR10a*, *miR10b,* and *miR-20a* in our mice model remains to be elucidated, we demonstrated that NPMc$^+$ specifically promotes this phenomenon, because we were able to reproduce it in a nonhematopoietic cell line using overexpression experiments.

miR10a is located within the *HOXB* cluster and is coexpressed with *HOXB4* and *HOXB5* through a common transcriptional mechanism in developing mouse embryos.[39] Similarly to patients with *NPM1*-mutated AML,[7] we observed a strong association between up-regulation of *miR10a* and increased *HOXB4* and *HOXB5* expression in BM cells from mice harboring the *NPM1* mutation A. This finding suggests that expression of this miRNA may be modulated by *cis* elements that also regulate *HOX* genes.[43] Another possible explanation is that in our setting, the cytoplasmic NPM1 mutant and/or delocalized wild-type NPM1 may increase *miR10a*, *miR10b,* and *miR20a* stabilization, boosting their expression levels. This is not surprising because NPM1 is involved in shuttling RNAs and ribosomal proteins to the cytosol,[44] and this shuttling mechanism may be relevant to a possible role in miRNA packaging, export, and stabilization. Interestingly, the NPM1 protein can bind miRNAs and

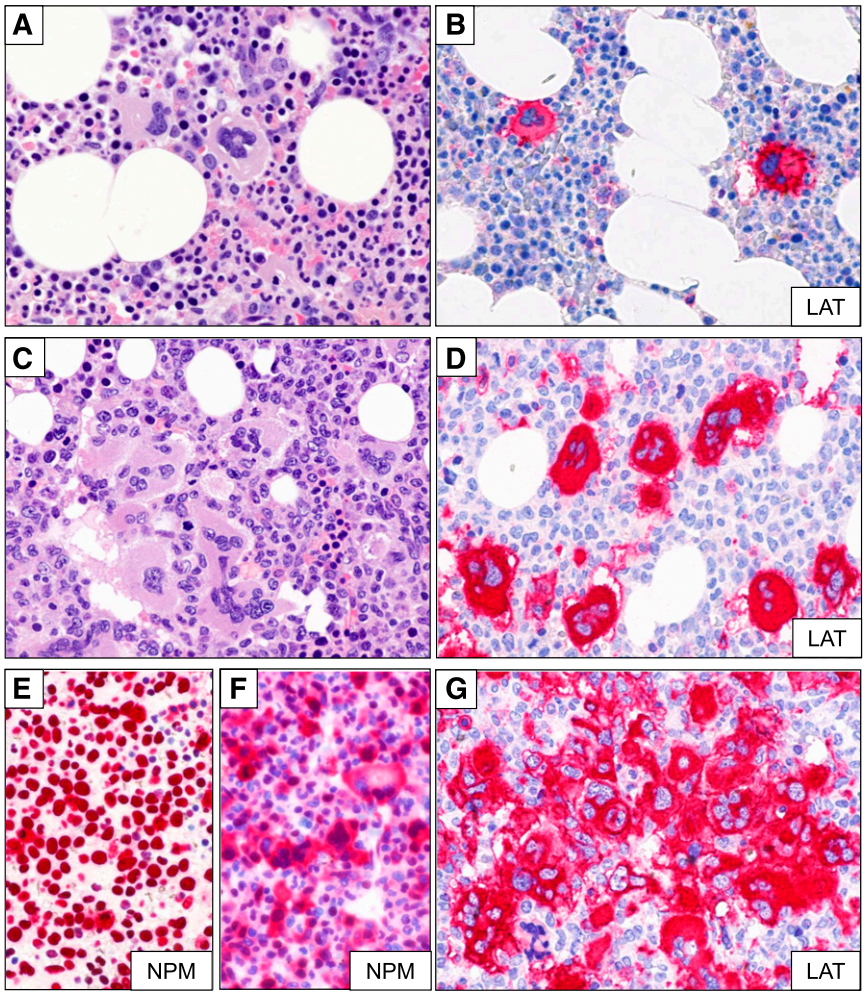

Figure 7. Megakaryocytes expansion in BM biopsy of *NPM1*-mutated AML patients. (A-B) Representative BM sections from a nonleukemic control were stained with (A) hematoxylin and eosin and (B) an anti-LAT antibody. (C-D) BM trephine sections from an *NPM1*-mutated AML patient with an increased number of megakaryocytes (~20 megakaryocytes ×40 field) as assessed by (C) hematoxylin and eosin and (D) immunostaining for human LAT. (E) Nucleus-restricted NPM1 expression in a representative *NPM1*-unmutated AML patient. (F) Aberrant cytoplasmic expression of NPM1 in dysplastic megakaryocytes (original magnification, ×40) of an *NPM1*-mutated AML patient. (G) LAT positive megakaryocytes in a representative *NPM1*-mutated AML patient with a megakaryocytes concentration >40 per ×40 field (original magnification, ×40).

protect them from degradation.[45] Indeed, mature cytoplasmic *miR10a* and *miR10b* up-regulation was accompanied by reduced miRNA precursor expression in mutant mice. This finding further supports the hypothesis that altered miRNA expression could be directly related to miRNA stabilization promoted by $NPMc^+$ expression rather than a consequence of immature $CD41^+$ megakaryocytes accumulation.

In our mouse model, we did not observe the onset of leukemia after a 1.5-year follow-up, corroborating the idea that the cytoplasmic NPM1 mutant is necessary but not a sufficient genetic lesion to cause AML. These results confirm previous findings in a transgenic $NPMc^+$ mice model[24] and are consistent with the concept that, similarly to other human cancers,[46] the development of AML results from >1 oncogenic hit.[47] For example, in the *NPM1*-mutated knock-in mouse model reported by Vassiliou et al,[26] one-third of mice developed delayed-onset AML requiring cooperating mutations. In leukemic patients, the NPM1 mutant may act synergistically with *FLT3-ITD*, *IDH1,* and/or *DNMT3A* mutations, which frequently associate with *NPM1*-mutated AML.[48-50] In this model, the *NPM1* mutation is likely to represent the initiating genetic event, and the other mutations are secondary alterations related to tumor progression.

In summary, we demonstrated for the first time that the expression of the NPM1 mutant results in the direct generation of signals determining a block of megakaryocytic development. Importantly, the phenotype of these mice recalls some features of human *NPM1*-mutated AML. Thus, our mouse model further expands the knowledge on the role of NPM1 mutant in leukemogenesis and may serve as an additional tool for investigating the cooperation between mutations affecting *NPM1* and other genes.

Acknowledgments

The authors thank Roberta Pacini and Alessia Tabarrini for performing immunohistochemical staining and Dr Luigi De Angelis for laboratory assistance. The authors also thank Claudia Tibidò for excellent secretarial assistance.

This work was supported by the Associazione Italiana Ricerca Cancro, the Associazione Umbra contro le Leucemie e i Linfomi, Fondazione Cassa di Risparmio di Perugia (grant 2010.011.0391), and Italian Minister of Health Project "Ricerca Finalizzata 2008" (grant RF-UMB-2008-1142331).

Authorship

Contribution: P.S. designed and performed experiments, analyzed and interpreted the data, and wrote the manuscript; E.V. performed experiments, analyzed and interpreted the data, and contributed to the writing of the paper; R.R. performed experiments on protein expression of the NPM1 mutant; O.B. and D.C. performed flow

cytometry; I.G. performed experiments on protein expression; N.B. contributed by generating the mouse model and writing the manuscript; T.I., P.Z., and A.M. provided clinical data on AML patients; E.T., M.P.M., F.F., and M.F.M. contributed to the writing of the manuscript; and B.F. led the project, provided expert hematopathologic analysis, supervised the study, and wrote the manuscript.

Conflict-of-interest disclosure: B.F. applied for a patent on the clinical use of NPM1 mutants. The remaining authors declare no competing financial interests.

Correspondence: Brunangelo Falini or Paolo Sportoletti, Institute of Hematology, University of Perugia, Ospedale S. Maria della Misericordia, S. Andrea delle Fratte, 06132 Perugia, Italy; e-mail: faliniem@unipg.it or sportolp@gmail.com.

References

1. Falini B, Mecucci C, Tiacci E, et al; GIMEMA Acute Leukemia Working Party. Cytoplasmic nucleophosmin in acute myelogenous leukemia with a normal karyotype. *N Engl J Med.* 2005; 352(3):254-266.
2. Falini B, Nicoletti I, Bolli N, et al. Translocations and mutations involving the nucleophosmin (NPM1) gene in lymphomas and leukemias. *Haematologica.* 2007;92(4):519-532.
3. Schlenk RF, Döhner K, Krauter J, et al; German-Austrian Acute Myeloid Leukemia Study Group. Mutations and treatment outcome in cytogenetically normal acute myeloid leukemia. *N Engl J Med.* 2008;358(18):1909-1918.
4. Haferlach C, Mecucci C, Schnittger S, et al. AML with mutated NPM1 carrying a normal or aberrant karyotype show overlapping biologic, pathologic, immunophenotypic, and prognostic features. *Blood.* 2009;114(14):3024-3032.
5. Alcalay M, Tiacci E, Bergomas R, et al. Acute myeloid leukemia bearing cytoplasmic nucleophosmin (NPMc+ AML) shows a distinct gene expression profile characterized by up-regulation of genes involved in stem-cell maintenance. *Blood.* 2005;106(3):899-902.
6. Verhaak RG, Wouters BJ, Erpelinck CA, et al. Prediction of molecular subtypes in acute myeloid leukemia based on gene expression profiling. *Haematologica.* 2009;94(1):131-134.
7. Garzon R, Garofalo M, Martelli MP, et al. Distinctive microRNA signature of acute myeloid leukemia bearing cytoplasmic mutated nucleophosmin. *Proc Natl Acad Sci USA.* 2008; 105(10):3945-3950.
8. Jongen-Lavrencic M, Sun SM, Dijkstra MK, Valk PJ, Löwenberg B. MicroRNA expression profiling in relation to the genetic heterogeneity of acute myeloid leukemia. *Blood.* 2008;111(10):5078-5085.
9. Becker H, Marcucci G, Maharry K, et al. Favorable prognostic impact of NPM1 mutations in older patients with cytogenetically normal de novo acute myeloid leukemia and associated gene- and microRNA-expression signatures: a Cancer and Leukemia Group B study. *J Clin Oncol.* 2010;28(4):596-604.
10. Russ AC, Sander S, Lück SC, et al. Integrative nucleophosmin mutation-associated microRNA and gene expression pattern analysis identifies novel microRNA - target gene interactions in acute myeloid leukemia. *Haematologica.* 2011; 96(12):1783-1791.
11. Martelli MP, Pettirossi V, Thiede C, et al. CD34+ cells from AML with mutated NPM1 harbor cytoplasmic mutated nucleophosmin and generate leukemia in immunocompromised mice. *Blood.* 2010;116(19):3907-3922.
12. Falini B, Martelli MP, Bolli N, Sportoletti P, Liso A, Tiacci E, Haferlach T. Acute myeloid leukemia with mutated nucleophosmin (NPM1): is it a distinct entity? *Blood.* 2011;117(4):1109-1120.
13. Arber DA, Brunning RD, Le Beau MM, et al. Acute myeloid leukaemia with recurrent genetic abnormalities. In: Swerdlow SH, Campo E, Harris NL, et al, eds. *WHO Classification of Tumours of Haematopoietic and Lymphoid Tissues.* Lyon, France: International Agency for Research on Cancer; 2008:110-123.
14. Borer RA, Lehner CF, Eppenberger HM, Nigg EA. Major nucleolar proteins shuttle between nucleus and cytoplasm. *Cell.* 1989;56(3):379-390.
15. Cordell JL, Pulford KA, Bigerna B, et al. Detection of normal and chimeric nucleophosmin in human cells. *Blood.* 1999;93(2):632-642.
16. Falini B, Bolli N, Shan J, et al. Both carboxy-terminus NES motif and mutated tryptophan(s) are crucial for aberrant nuclear export of nucleophosmin leukemic mutants in NPMc+ AML. *Blood.* 2006;107(11):4514-4523.
17. Bolli N, Nicoletti I, De Marco MF, et al. Born to be exported: COOH-terminal nuclear export signals of different strength ensure cytoplasmic accumulation of nucleophosmin leukemic mutants. *Cancer Res.* 2007;67(13):6230-6237.
18. Falini B, Bolli N, Liso A, Martelli MP, Mannucci R, Pileri S, Nicoletti I. Altered nucleophosmin transport in acute myeloid leukaemia with mutated NPM1: molecular basis and clinical implications. *Leukemia.* 2009;23(10):1731-1743.
19. Falini B, Martelli MP, Bolli N, et al. Immunohistochemistry predicts nucleophosmin (NPM) mutations in acute myeloid leukemia. *Blood.* 2006;108(6):1999-2005.
20. Bolli N, De Marco MF, Martelli MP, et al. A dose-dependent tug of war involving the NPM1 leukaemic mutant, nucleophosmin, and ARF. *Leukemia.* 2009;23(3):501-509.
21. Colombo E, Martinelli P, Zamponi R, et al. Delocalization and destabilization of the Arf tumor suppressor by the leukemia-associated NPM mutant. *Cancer Res.* 2006;66(6):3044-3050.
22. Bonetti P, Davoli T, Sironi C, Amati B, Pelicci PG, Colombo E. Nucleophosmin and its AML-associated mutant regulate c-Myc turnover through Fbw7 gamma. *J Cell Biol.* 2008;182(1):19-26.
23. Leong SM, Tan BX, Bte Ahmad B, et al. Mutant nucleophosmin deregulates cell death and myeloid differentiation through excessive caspase-6 and -8 inhibition. *Blood.* 2010;116(17):3286-3296.
24. Cheng K, Sportoletti P, Ito K, Clohessy JG, Teruya-Feldstein J, Kutok JL, Pandolfi PP. The cytoplasmic NPM mutant induces myeloproliferation in a transgenic mouse model. *Blood.* 2010;115(16):3341-3345.
25. Bolli N, Payne EM, Grabher C, et al. Expression of the cytoplasmic NPM1 mutant (NPMc+) causes the expansion of hematopoietic cells in zebrafish. *Blood.* 2010;115(16):3329-3340.
26. Vassiliou GS, Cooper JL, Rad R, et al. Mutant nucleophosmin and cooperating pathways drive leukemia initiation and progression in mice. *Nat Genet.* 2011;43(5):470-475.
27. Okabe M, Ikawa M, Kominami K, Nakanishi T, Nishimune Y. 'Green mice' as a source of ubiquitous green cells. *FEBS Lett.* 1997;407(3):313-319.
28. Lakso M, Sauer B, Mosinger B Jr, et al. Targeted oncogene activation by site-specific recombination in transgenic mice. *Proc Natl Acad Sci USA.* 1992;89(14):6232-6236.
29. Martelli MP, Manes N, Liso A, et al. A western blot assay for detecting mutant nucleophosmin (NPM1) proteins in acute myeloid leukaemia. *Leukemia.* 2008;22(12):2285-2288.
30. Quentmeier H, Martelli MP, Dirks WG, et al. Cell line OCI/AML3 bears exon-12 NPM gene mutation-A and cytoplasmic expression of nucleophosmin. *Leukemia.* 2005;19(10):1760-1767.
31. Pronk CJ, Rossi DJ, Månsson R, et al. Elucidation of the phenotypic, functional, and molecular topography of a myeloerythroid progenitor cell hierarchy. *Cell Stem Cell.* 2007;1(4):428-442.
32. Facchetti F, Chan JK, Zhang W, et al. Linker for activation of T cells (LAT), a novel immunohistochemical marker for T cells, NK cells, mast cells, and megakaryocytes: evaluation in normal and pathological conditions. *Am J Pathol.* 1999;154(4):1037-1046.
33. Sola-Visner MC, Christensen RD, Hutson AD, Rimsza LM. Megakaryocyte size and concentration in the bone marrow of thrombocytopenic and nonthrombocytopenic neonates. *Pediatr Res.* 2007;61(4):479-484.
34. Kühn R, Schwenk F, Aguet M, Rajewsky K. Inducible gene targeting in mice. *Science.* 1995; 269(5229):1427-1429.
35. Gorello P, Cazzaniga G, Alberti F, et al. Quantitative assessment of minimal residual disease in acute myeloid leukemia carrying nucleophosmin (NPM1) gene mutations. *Leukemia.* 2006;20(6):1103-1108.
36. Zhang J, Varas F, Stadtfeld M, Heck S, Faust N, Graf T. CD41-YFP mice allow in vivo labeling of megakaryocytic cells and reveal a subset of platelets hyperreactive to thrombin stimulation. *Exp Hematol.* 2007;35(3):490-499.
37. Garzon R, Pichiorri F, Palumbo T, et al. MicroRNA fingerprints during human megakaryocytopoiesis. *Proc Natl Acad Sci USA.* 2006;103(13):5078-5083.
38. Opalinska JB, Bersenev A, Zhang Z, et al. MicroRNA expression in maturing murine megakaryocytes. *Blood.* 2010;116(23):e128-e138.
39. Mansfield JH, Harfe BD, Nissen R, et al. MicroRNA-responsive 'sensor' transgenes uncover Hox-like and other developmentally regulated patterns of vertebrate microRNA expression. *Nat Genet.* 2004;36(10):1079-1083.
40. Cheng K, Grisendi S, Clohessy JG, Majid S, Bernardi R, Sportoletti P, Pandolfi PP. The leukemia-associated cytoplasmic nucleophosmin mutant is an oncogene with paradoxical functions: Arf inactivation and induction of cellular senescence. *Oncogene.* 2007;26(53):7391-7400.
41. Pasqualucci L, Liso A, Martelli MP, et al. Mutated nucleophosmin detects clonal multilineage involvement in acute myeloid leukemia: Impact on WHO classification. *Blood.* 2006;108(13):4146-4155.
42. Falini B, Macijewski K, Weiss T, et al. Multilineage dysplasia has no impact on biologic, clinicopathologic, and prognostic features of AML with mutated nucleophosmin (NPM1). *Blood.* 2010;115(18):3776-3786.
43. Tanzer A, Amemiya CT, Kim CB, Stadler PF. Evolution of microRNAs located within Hox gene clusters. *J Exp Zoolog B Mol Dev Evol.* 2005; 304(1):75-85.
44. Grisendi S, Mecucci C, Falini B, Pandolfi PP. Nucleophosmin and cancer. *Nat Rev Cancer.* 2006;6(7):493-505.

45. Wang K, Zhang S, Weber J, Baxter D, Galas DJ. Export of microRNAs and microRNA-protective protein by mammalian cells. *Nucleic Acids Res.* 2010;38(20):7248-7259.

46. Stratton MR, Campbell PJ, Futreal PA. The cancer genome. *Nature.* 2009;458(7239):719-724.

47. Gilliland DG. Hematologic malignancies. *Curr Opin Hematol.* 2001;8(4):189-191.

48. Falini B, Sportoletti P, Martelli MP. Acute myeloid leukemia with mutated NPM1: diagnosis, prognosis and therapeutic perspectives. *Curr Opin Oncol.* 2009;21(6):573-581.

49. Marcucci G, Haferlach T, Döhner H. Molecular genetics of adult acute myeloid leukemia: prognostic and therapeutic implications. *J Clin Oncol.* 2011;29(5):475-486.

50. Takahashi S. Current findings for recurring mutations in acute myeloid leukemia. *J Hematol Oncol.* 2011;4:36.